USGS
science for a changing world

Prepared in cooperation with Portland State University

# Results of Hydrologic Monitoring of a Landslide-Prone Hillslope in Portland's West Hills, Oregon, 2006–2017

Data Series 1050

U.S. Department of the Interior
U.S. Geological Survey

**Cover.** The photograph shows terrain and vegetation in the vicinity of the monitoring site in Portland's West Hills, Oregon. The camera was facing northeast and located about 50-meters southeast of the hydrologic monitoring site. The solar panel and a rain gage can be seen in the foreground. The treeless area is a scar from a recent landslide; the zone of depression was filled with gravel to mitigate the disturbed topography.

# Results of Hydrologic Monitoring of a Landslide-Prone Hillslope in Portland's West Hills, Oregon, 2006–2017

By Joel B. Smith, Jonathan W. Godt, Rex L. Baum, Jeffrey A. Coe, William L. Ellis, Eric S. Jones, and Scott F. Burns

Prepared in cooperation with Portland State University

Data Series 1050

**U.S. Department of the Interior**
**U.S. Geological Survey**

**U.S. Department of the Interior**
RYAN K. ZINKE, Secretary

**U.S. Geological Survey**
William H. Werkheiser, Acting Director

U.S. Geological Survey, Reston, Virginia: 2017



Suggested citation:
Smith, J.B., Godt, J.W., Baum, R.L., Coe, J.A., Ellis, W.L., Jones, E.S., and Burns, S.F., 2017, Results of hydrologic monitoring of a landslide-prone hillslope in Portland's West Hills, Oregon, 2006–2017: U.S. Geological Survey Data Series 1050, 10 p., https://doi.org/10.3133/ds1050.

ISSN 2327-638X (online)

# Contents



## Figures



## Tables

# Conversion Factors

International System of Units to Inch/Pound

| Multiply | By | To obtain |
|---|---|---|
| | Length | |
| millimeter (mm) | 0.03937 | inch (in.) |
| meter (m) | 3.281 | foot (ft) |
| kilometer (km) | 0.6214 | mile (mi) |
| | Pressure | |
| kilopascal (kPa) | 0.009869 | atmosphere, standard (atm) |
| kilopascal (kPa) | 0.1450 | pound per square inch ($lb/ft^2$) |
| | Volume | |
| cubic meter ($m^3$) | 1.308 | cubic yard ($yd^3$) |

Temperature in degrees Celsius (°C) may be converted to degrees Fahrenheit (°F) as

$$°F = (1.8 \times °C) + 32.$$

Temperature in degrees Fahrenheit (°F) may be converted to degrees Celsius (°C) as

$$°C = (°F - 32) / 1.8.$$

## Datum

Vertical coordinates are referenced to the North American Vertical Datum of 1988 (NAVD 88).

Altitude, as used in this report, refers to distance above the vertical datum.

Horizontal coordinate information is referenced to the Universal Transverse Mercator, Zone 10, meters.

# Results of Hydrologic Monitoring of a Landslide-Prone Hillslope in Portland's West Hills, Oregon, 2006–2017

By Joel B. Smith,[1] Jonathan W. Godt,[1] Rex L. Baum,[1] Jeffrey A. Coe,[1] William L. Ellis,[1] Eric S. Jones,[1] and Scott F. Burns[2]

## Abstract

The West Hills of Portland, in the southern Tualatin Mountains, trend northwest along the west side of Portland, Oregon. These silt-mantled mountains receive significant wet-season precipitation and are prone to sliding during wet conditions, occasionally resulting in property damage or casualties. In an effort to develop a baseline for interpretive analysis of the groundwater response to rainfall, an automated monitoring system was installed in 2006 to measure rainfall, pore-water pressure, soil suction, soil-water potential, and volumetric water content at 15-minute intervals. The data show a cyclical pattern of groundwater and moisture content levels—wet from October to May and dry between June and September. Saturated soil conditions tend to last throughout the wet season. These data show the hydrologic response of the monitored area to rainfall and provide insight into the dynamics of rainfall-initiated landsliding. This report details the monitoring methods and presents data collected from January 10, 2006, through January 23, 2017.

## Introduction

Quantification of the hydrologic response of a hillslope to precipitation is requisite for increased accuracy in the prediction of rainfall-induced landsliding (for example, Reid and others, 2008). Hydrologic conditions of a hillslope are somewhat transient in comparison to most other physical aspects of a hillslope and are subject to the hysteretic process of drying or wetting (Lu and Godt, 2013). As the moisture content in a hillslope soil changes, so does the strength of the soil and the ability of the slope to resist sliding. Given the dynamic and nonisotropic aspects of a "typical" hillslope, long-term measurements with electronic sensors bolster theoretical analyses and may lead to increased landslide-predictive ability. In this report, we review background information related to landslide monitoring in Portland's West Hills, describe site details and give technical details of the instruments used at this monitoring site, and present processed data from the monitoring site (Smith and others, 2017).

## Physiographic Setting

### Climatic Relationship to Landslides

Pore-pressure conditions sufficient to cause a destabilizing soil strength reduction are usually attributed to high-intensity storm events occurring after antecedent conditions for landsliding have been met (for example, Wiley, 2000). Such antecedent conditions are usually met multiple times during the typical wet winters in Portland.

Statistical analysis of data from the National Weather Service monitoring station located at the Portland Airport (Portland WSO AP), from the years 1941 to 2012, defines average, minimum, and maximum monthly precipitation and average snowfall for the region. The Portland WSO AP is located about 12 kilometers east-northeast from the West Hills monitoring site and stands about 6 meters (m) above mean sea level. The elevation of the West Hills monitoring site, by comparison, is about 300 m above mean sea level. Precipitation is directly correlated with elevation during any given storm event (Taylor and Bartlett, 1993), so the values depicted in figure 1 are likely lower than the precipitation occurring at the West Hills monitoring site because greater rainfall is expected at higher elevations. November, December, and January are the wettest months with about 45 percent of the average annual precipitation. October and February receive similar yet smaller amounts of rainfall, but February has a greater chance of landslide occurrence than October because of higher antecedent moisture conditions and greater potential for rain-on-snow events.

On average, the snow water equivalent of snowfall during the months of November through March totals about 135 millimeters (mm). According to Harr (1981), snowmelt during periods of prolonged rainfall (a rain-on-snow event) is a major contributing factor to landsliding in western Oregon. Snowpacks in western Oregon are considered "warm," unlike those in the Rocky

[1]U.S. Geological Survey.

[2]Portland State University Department of Geology.

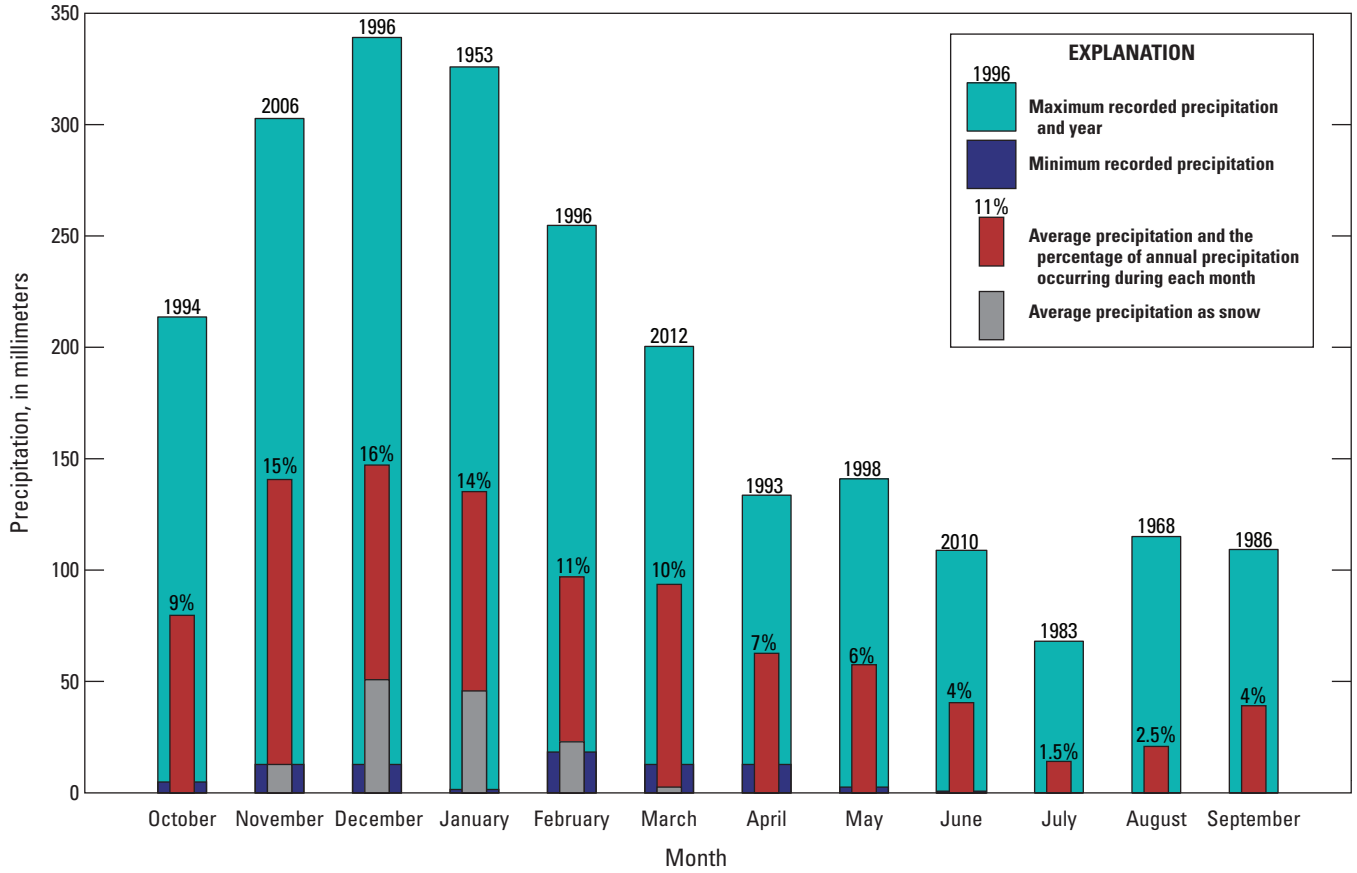


**Figure 1.** Monthly precipitation statistics recorded from 1940 to 2013 at the National Weather Service monitoring station at Portland Airport. Shown also are years with the maximum precipitation and the percentage of average annual precipitation during each month.

Mountains, and require very little energy to melt (Smith, 1974). The interior temperature of a warm snowpack is at or near 0 degrees Celsius (ºC) and is able to release a very high quantity of water as a result of heat transfer from rain. There are several well-documented instances of rain-on-snow events in western Oregon (for example, Dyrness, 1967; Burns and others, 1998).

Annual precipitation ranges from about 600 mm to about 1,600 mm with a mean of 937 mm (fig. 2). Given records of historical landsliding, elevated annual precipitation correlates well with landslide occurrence. However, this proportionality decreases under certain conditions. For example, if a greater than usual amount of rainfall occurs in the early season before antecedent conditions have been met, there may be relatively few landslides during a year with above-average precipitation. Similarly, a year that only receives a moderate amount of rainfall early season followed by intense storms in late season might experience large numbers of landslides with only an average amount of annual rainfall.

## Historical Landsliding in the West Hills

During the winter of 1996, the Portland area (and other parts of western Oregon) experienced a large rain-on-snow storm event (Taylor, 1997) that generated flooding and widespread landslides. Burns and others (1998) identified 705 distinct instances of landsliding in the Portland area because of the storm event. Burns and others (1998) also delineated four regions, or landslide provinces, to characterize the geology found where 75 percent of the failures occurred (the remaining 25 percent occurred in noncategorized locations) along with the percentage of events that occurred in each—West Hills Silt Soil Province (53 percent), Debris Flows in Valley Bottoms Province (6.4 percent), Steep Bluffs Along the Rivers Province (5.7 percent), and the Fine-Grained Troutdale Formation Province (10 percent). The West Hills monitoring site is located within the West Hills Silt Soil Province.

Landslide events such as this one in 1996 are usually costly for the City of Portland and its associated municipalities and private-property owners. Landslide damage during the winter of 1996 cost the city an estimated $32.5 million (Oregon Department of Geology and Mineral Industries, 1996). Landslide damage resulting from a less extreme winter during 1955–56 cost the City of Portland $200,000 ($1.8 million adjusted for inflation as of 2015) including repair of the municipal water system, streets, and city parks (Schlicker, 1956).

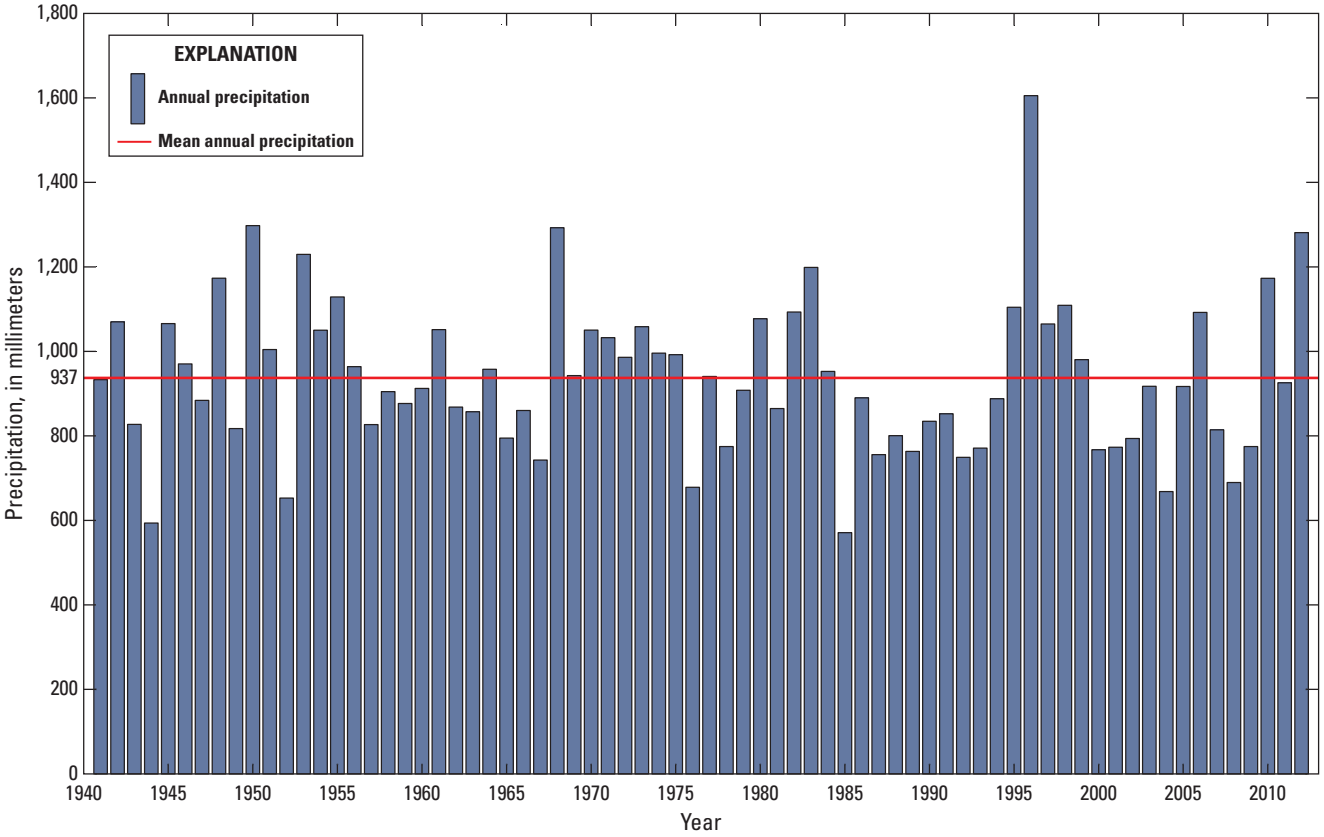


**Figure 2.** Annual precipitation amounts recorded from 1941 to 2012.

## Monitoring Site

The West Hills monitoring site is located about 180 m above Balch Creek on the moderately dissected western escarpment of Balch Creek canyon in the Balch Creek watershed. The site is about 5 kilometers west of downtown Portland on a northwest-facing, topographically divergent slope. The site is located on the forested perimeter of Mount Calvary Cemetery just north of a paved area and mausoleum. The mixed conifer forest vegetation at the site consists primarily of large evergreen trees and smaller hardwoods. The shade from the canopy is sufficient to keep understory vegetation relatively thin. The ground surface is covered with plant litter.

Reese and others (2007) reported a January 2006 landslide on the premises, about 500 meters southwest of the monitoring site on a northeast-facing hillslope. In addition, Reese and others (2007) attributed the failure to an unusually wet winter before the slide and fill loading at the slope crest.

## Site Geology

A geologic map by Beeson and others (1991) shows the monitoring site (fig. 3) near the contact between a basaltic-andesite Boring Lava originating from the Elk Point vent (Pliocene to Pleistocene, less than about 2.5 mega-annum [Ma]) and the Sentinel Bluffs Member of Grande Ronde Basalt of Columbia River Basalt Group (middle Miocene [17–6 Ma]) basaltic lava flow. The volcanic hillslopes have been complexly faulted (Walsh and others, 2011) and shaped by gravity-driven, mass-wasting processes. The younger Boring Lava formation (Treasher, 1942; Allen, 1975) lying on top of the Sentinel Bluffs unit is more resistant to weathering than the older material and has caused an over-steepening of the slopes (Trimble, 1963).

The over-steepened hillslopes flanking the Portland Basin were subsequently mantled in loess (25 to 13 ka [kilo-annum] [Madin and others, 2008]). The silt was deposited as a shallow layer in an unconsolidated state. Furthermore, the silt was dry when it was originally deposited and experiences relatively high-strength loss when saturated. The depth of the loess is variable, from 1 to 30 m, and inversely related to the local slope angle. As many as four thin, lower-permeability soil horizons occur within the loess that may serve as discrete failure surfaces. The less permeable layers are believed to be the contact points between buried soils, as the aeolian deposition occurred in distinct episodes interspersed with soil development (Lentz, 1981; Evarts and others, 2009).

Left undisturbed, the loess is in equilibrium with gravity and internal forces resisting downhill movement. Disturbances such as rapid soil saturation, ground motion (Madin, 1998), or even tree wind-throw can quickly upset the balance, as can human activity (Swanston, 1974). Most of the forestland located within Portland's West Hills has been selectively logged or clearcut (City of Portland, 1991) and has not yet returned to vegetative equilibrium.

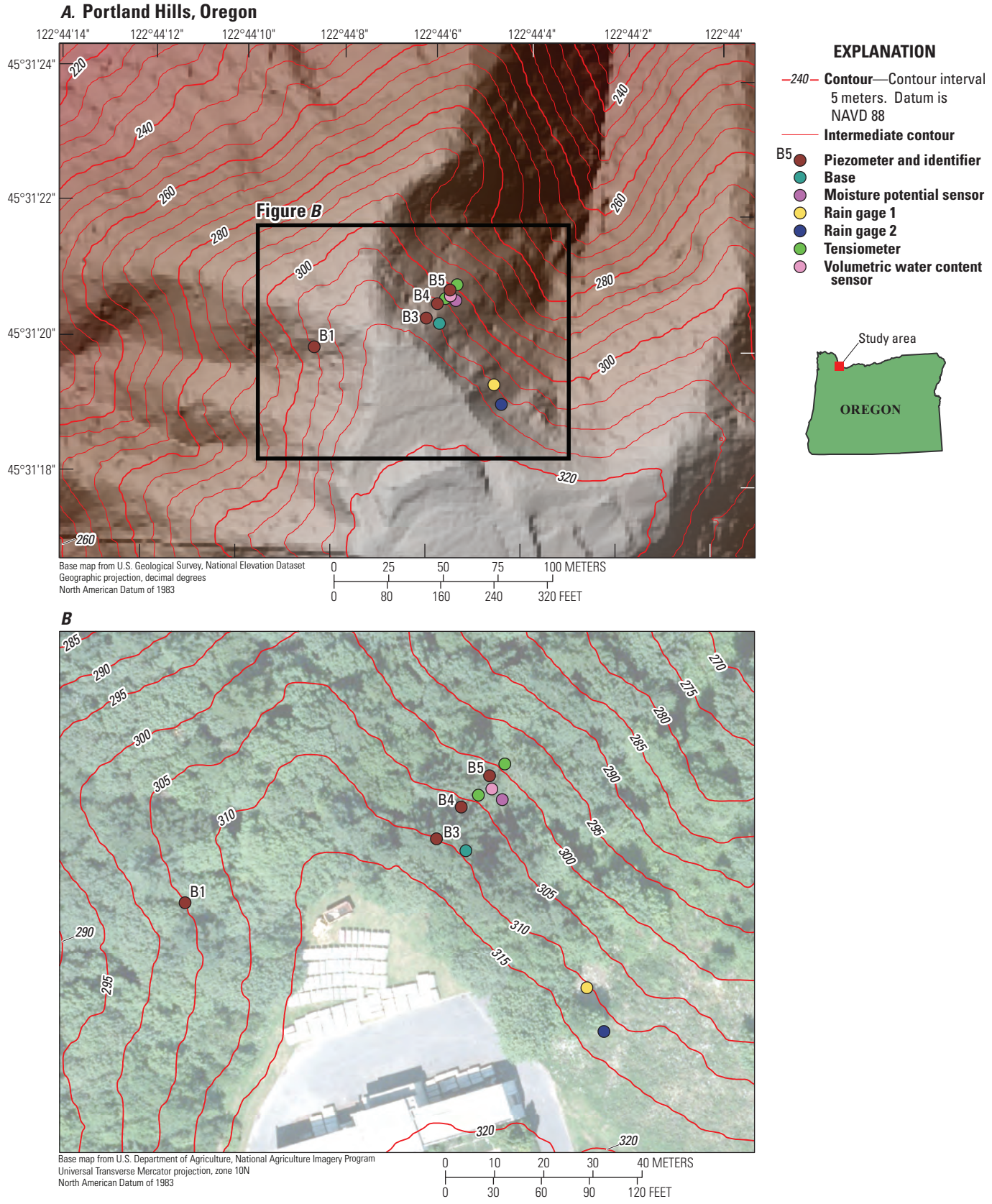


**Figure 3.** Shaded hillslope (*A*) within site vicinity and showing contours and (*B*) instrument locations. Labels B1–B5 correspond to the piezometer borehole locations. Borehole 2 is not shown; it was not used for monitoring purposes because of the presence of very shallow weathered basalt.

Burns and others (1998) identified the West Hills Silt Soil Province as the most frequent landslide producer in the Portland area. The Natural Resources Conservation Services Web Soil Survey (U.S. Department of Agriculture Natural Resources Conservation Service, 2014) classifies soils in the Mount Calvary Cemetery area as "Goble" silt loam. Goble soils are moderately well drained above and between paleosol layers, but the layer contacts have low permeability. These soils are on slopes (locally) of 30 to 60 percent (15 to 30 degrees). Redfern (1976) identified Tualatin mountain slopes steeper than 30 percent (15 degrees) as having severe landslide potential while noting that about 75 percent of Portland's uplands exceed this slope angle.

According to Burns and others (1998), the slides from the 1996 event in the West Hills were mostly small, complex rotational earth slides-earth flows (for example, Varnes, 1978) with volumes that ranged from 20 to 400 cubic meters. Potential failure surfaces for the landslides included the loess paleosols and the contact between the loess and underlying units (Madin and others, 2008). Madin and others (2008) also identified landslide deposits in the Linnton quadrangle (due west) and described their shapes as 1.5–3 m thick with arcuate headscarps and bulging "toes." The deposits also included smaller internal arcuate scarps and typical hummocky surfaces. Four percent of the surface area of the Linnton quadrangle is covered by some form of landslide deposit (Madin and others, 2008).

# Methods

The near-real-time data acquisition system at the Portland Hills site is equipped with meteorological and subsurface hydrologic monitoring instrumentation and is controlled by a central data logger. The site is powered by a 50-watt solar panel with a 55 ampere-hour sealed lead acid battery and 6-ampere charging current regulator. Remote two-way communications with the data logger are enabled with a static IP modem transmitting on a cellular network. These communications allow remote data retrieval from U.S. Geological Survey offices in Golden, Colo., as well as the ability to modify the control program running on the data logger.

The data acquisition system has undergone several changes since coming online in January 2006 (table 1). The initial installment included a rain gage, an electronic piezometer, and three volumetric water content devices (with temperature sensors). The initial system was replaced with a long-term monitoring station in November 2006 that consisted of two rain gages, seven tensiometers (with temperature), and seven electronic borehole piezometers. Twelve volumetric water-content instruments were added in December 2007, and six moisture potential sensors were installed in October 2008.

**Table 1.** Chronological operating status of sensors. Ratio indicates number of operational sensors compared to installed sensors.

[RG, Rain gages; P, piezometers; VWC, volumetric water content sensors; T, tensiometers; and MP, moisture potential sensors]

| Portland Hills system status | | | | | | |
|---|---|---|---|---|---|---|
| **Preliminary installation** | | | | | | |
| **Date** | **RG** | **P** | **VWC** | | | **Comment** |
| 2006 January 10 | 1/1 | 1/1 | 3/3 | | | Initial site installation; all installed instruments operational. |
| 2007 January 25 | 0/1 | 0/1 | 0/3 | | | Initial site system decomissioned. |
| **Primary installation** | | | | | | |
| **Date** | **RG** | **T** | **P** | **VWC** | **MP** | **Comment** |
| 2006 November 9 | 2/2 | 7/7 | 7/7 | 0 | 0 | Initial site installation; all installed instruments operational. |
| 2007 December 14 | 2/2 | 7/7 | 7/7 | 11/11 | 0 | Added volumetric water content sensors. |
| 2007 June 22 | 0/2 | 0/7 | 0/7 | 0/11 | 0 | System offline; no data collected. |
| 2007 July 8 | 2/2 | 7/7 | 7/7 | 11/11 | 0 | System back online |
| 2008 February 27 | 2/2 | 6/7 | 7/7 | 11/11 | 0 | Pressure and temperature signals from tensiometer T3 at 93 centimeters (cm) become excessively noisy. |
| 2008 March 10 | 0/2 | 0/7 | 0/7 | 0/11 | 0 | System offline; no data collected. |
| 2008 March 30 | 2/2 | 6/7 | 7/7 | 11/11 | 0 | System back online. |
| 2008 August 30 | 2/2 | 6/7 | 5/7 | 11/11 | 0 | Piezometers in boreholes 3 and 5 become nonfunctional. |
| 2008 October 23 | 2/2 | 7/7 | 6/7 | 11/11 | 0 | Piezometer in borehole 3 resumes function. Noise in tensiometer T3 is resolved. |
| 2009 February 1 | 2/2 | 7/7 | 6/7 | 10/11 | 0 | Signal from volumetric water content instrument at 105 cm becomes noisy and unreliable. |
| 2009 November 17 | 2/2 | 7/7 | 5/7 | 10/11 | 0 | Piezometer in borehole 4 nonfunctional. |
| 2010 January 26 | 0/2 | 0/7 | 0/7 | 0/11 | 0 | System offline; no data collected. |
| 2010 February 5 | 2/2 | 7/7 | 5/7 | 10/11 | 0 | System back online. |
| 2010 February 9 | 2/2 | 7/7 | 5/7 | 10/11 | 6/6 | Moisture potential sensors installed and functioning nominally. |
| 2010 March 22 | 0/2 | 0/7 | 0/7 | 0/11 | 0/6 | System offline; no data collected. |
| 2010 November 14 | 2/2 | 7/7 | 5/7 | 10/11 | 6/6 | System back online. |
| 2011 October 27 | 2/2 | 7/7 | 1/7 | 10/11 | 6/6 | Four borehole piezometers disconnected from system. |
| 2010 January 15 | 2/2 | 6/7 | 1/7 | 10/11 | 6/6 | Tensiometer T2 at 156 cm begins to show occasional spikes. |
| 2013 October 29 | 2/2 | 5/7 | 1/7 | 10/11 | 6/6 | Tensiometer T4 at 157 cm damaged when refilling. |
| 2014 February 1 | 1/2 | 5/7 | 1/7 | 10/11 | 6/6 | Rain gage 1 signal lead chewed by rodent. |
| 2016 September 11 | 1/2 | 5/7 | 1/7 | 10/11 | 6/6 | Tensiometer T4 temperature sensor begins showing signal excursions. |

## Rain Gages

Two tipping-bucket rain gages (Hydrological Services Tipping Bucket Rain Gauge Model TB4), calibrated to 0.254 mm per tip, were installed in a cleared area on the hillslope (fig. 3). The rain gages were mounted on concrete pads about 0.1 m above ground level.

## Volumetric Water-Content Sensors

Ten volumetric water content (VWC) instruments (Decagon Devices EC–5 soil moisture sensors) were installed in a vertical profile in the uphill face of a soil pit (fig. 3). The sensors provide an indirect volumetric water content measurement by correlating the dielectric permittivity of the soil to VWC using a high-measurement frequency to filter salinity and textural effects (Kizito and others, 2008). The sensors are accurate to about 2 percent over a volume of about 0.24 liters in a wide range of soil types. Instrument depths are shown in table 2.

The VWC data provided have a linear conversion applied to the raw data. The raw data are the quotient of the output (dividend) and input (divisor) voltages. The linear conversion applied to the raw sensor output uses a multiplier of $1.19\times10^{-3}$ and an offset of $-4.0\times10^{-1}$. This conversion was processed in real-time at the time of acquisition.

## Tensiometers

Seven field-refillable tensiometers were installed at the site to provide a direct measurement of positive and negative water pressure. The instruments measure pore pressure over a range of 100 kilopascals (kPa) to –85 kPa (suction), are accurate to 0.05 kPa, and automatically compensate for barometric pressure fluctuations through a semipermeable pressure vent found in the cable jacket above ground. The tensiometers are located in two arrays (see fig. 3) with each array measuring pore pressure at various depths. An upper array contains four tensiometers (T1, T2, T3, T4) and the lower, located about 10 m downslope, comprises three (T5, T6, T7). The tensiometers were installed in hand-augered, 25-mm diameter boreholes tilted roughly normal to the slope. The boreholes were tilted in order to place the sensing tip of the instrument beneath undisturbed soil. The shallowest 25 centimeters (cm) of the boring was excavated to allow emplacement of a 3.8-cm, diameter-capped rigid polyvinyl chloride (PVC) pipe around the uppermost length of the tensiometer body. This housing was intended to protect the tensiometer's refill tubes and electrical connections while inhibiting surface-water infiltration around the shaft of the instrument. After installation, the PVC was grouted into place and the excavation backfilled. Figure 4 details a typical tensiometer installation, and table 3 provides specific details.

The data provided from the tensiometers may contain seasonally erroneous data because of cavitation (see fig. 5). The tensiometers use deaired water as a hydraulic medium to relay the pressure on the porous cup to a pressure transducer within the tensiometer body. During prolonged dry conditions (such as during the summer months), the deaired water within the tensiometer begins to cavitate, and it is gradually displaced by air. Initially, the tensiometer continues to function with reduced response time and range, but eventually the cup empties to the extent that a void (air bubble) begins to form

**Table 2.** Volumetric water content sensor and moisture potential sensor installation notes.

[VWC, volumetric water content; MP, moisture potential; m, meter]

| VWC sensor | MP sensor | Depth (m) | Notes |
|---|---|---|---|
| 1 | 1 | 0.20 | About the limit of dense root zone |
| 2 | | 0.30 | In silt |
| 3 | 2 | 0.40 | In silt |
| 4 | | 0.50 | In silt |
| 5 | 3 | 0.60 | Depth of possible paleosol layer; lighter and denser below, darker above |
| 6 | | 0.70 | In silt |
| 7 | 4 | 0.80 | In silt |
| 8 | | 0.90 | In silt |
| | 5 | 1.00 | In silt |
| 9 | | 1.05 | In silt |
| 10 | 6 | 1.20 | Near the contact between basalt and silt |
| 11 | | 1.30 | In weathered basalt |

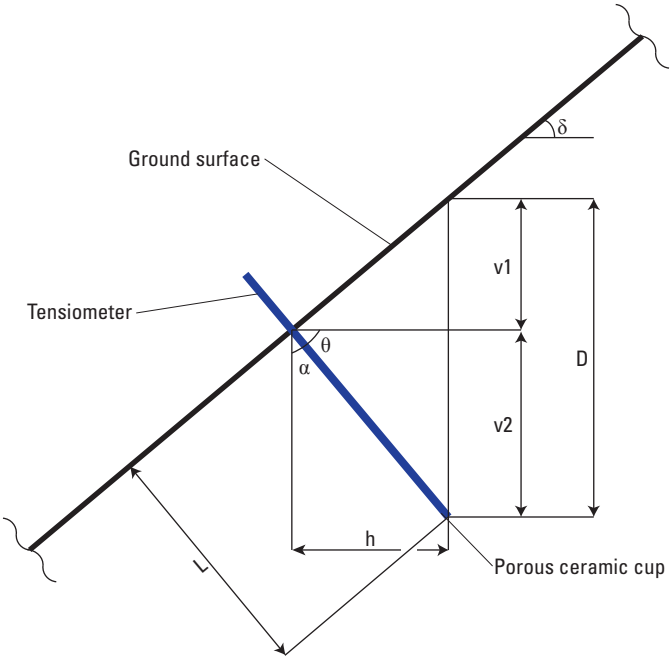


**Figure 4.** Tensiometer installation geometry (protective housing not shown). Depths, or D, for each tensiometer are listed in table 3. (δ, local slope; L, slope normal depth of tensiometer; θ, tensiometer plunge; α, tensiometer inclination; v1, vertical distance above the intersection of the tensiometer and ground surface to the ground surface above the tensiometer tip; v2, vertical distance below the intersection of the tensiometer and ground surface to the tensiometer tip; D, depth of the tensiometer tip beneath the ground surface)

**Table 3.** Tensiometer installation information. See figure 4 for installation geometry.

[δ, local slope; L, slope normal depth of tensiometer; θ, tensiometer plunge; α, tensiometer inclination; v1, vertical distance above the intersection of the tensiometer and ground surface to the ground surface above the tensiometer tip; h, horizontal distance between the intersection of the tensiometer and ground surface and the ground surface above the tensiometer tip; v2, vertical distance below the intersection of the tensiometer and ground surface to the tensiometer tip; D, depth of the tensiometer tip beneath the ground surface; I.D., identification; cm, centimeters]

| Tensiometer I.D. | Array location | δ (degrees) | L (cm) | θ (degrees) | α (degrees) | v1 (cm) | h (cm) | v2 (cm) | D (cm) |
|---|---|---|---|---|---|---|---|---|---|
| T1 | a1 | 31 | 63 | 117 | 27 | 56 | 29 | 17 | 73 |
| T2 | a1 | 31 | 80 | 122 | 32 | 68 | 42 | 25 | 93 |
| T3 | a1 | 31 | 134 | 122 | 32 | 114 | 71 | 43 | 156 |
| T4 | a1 | 31 | 178 | 118 | 28 | 157 | 84 | 50 | 207 |
| T5 | a2 | 24 | 80 | 125 | 35 | 66 | 46 | 20 | 86 |
| T6 | a2 | 24 | 143 | 113 | 23 | 132 | 56 | 25 | 157 |
| T7 | a2 | 24 | 195 | 110 | 20 | 183 | 67 | 30 | 213 |

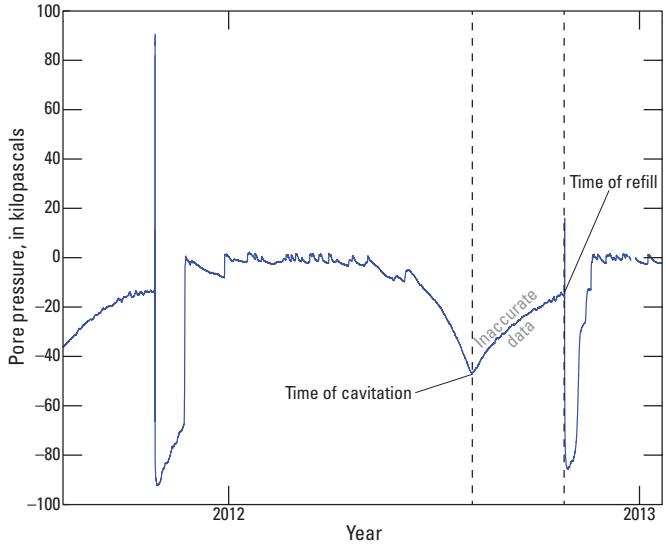


**Figure 5.** Tensiometer cavitation example. The plot shows the annual cycle and timing of tensiometer cavitation and refill. The tensiometer data collected between time of cavitation and the time of refill does not reflect actual pore-pressure values.

around the internal pressure transducer, and the sensor's readings slowly begin to approach a reading of neutral pore pressure—no longer reading actual pore-pressure values. Because of this inherent design limitation, the instrument is intended to be manually refilled. The instruments described in this report have been refilled at the onset of the annual wet season, usually around late October. The time of cavitation is usually apparent when viewing the data; it occurs simultaneously with a sensor's minimum pressure reading and is followed by an increase in pore pressure in the absence of any monitored rainfall.

## Moisture Potential Sensors

An array of six Decagon Devices MPS-1 moisture potential sensors was installed in the uphill face of a soil pit to measure soil suction along a vertical profile. The six sensors are installed in 20-cm increments from 20 to 120 cm below the ground surface (see table 2). The moisture potential sensors have a range from –10 kPa to –500 kPa with a resolution of about 1 to 4 kPa at low to high suctions, respectively. The accuracy of the sensor is about 5 kPa from –10 to –50 kPa and about 20 percent of reading from –50 to –500 kPa. The sensor measures moisture potential indirectly by correlating moisture potential to the simultaneous dielectric permittivity of an embedded ceramic disk.

## Piezometers

Seven vibrating-wire (VW) piezometers were installed at the site to measure pore pressure. Four VW piezometers were placed at various depths in borehole one (B1) and the others in borehole three (B3), borehole four (B4), and borehole five (B5), respectively. Borehole two (B2) contained weathered basalt (bedrock) near the ground surface and was abandoned. The holes were bored using 5.7-cm tooling driven by a demolition hammer. The piezometers in B1 were installed using a fully grouted method (Mikkelsen and Green, 2003). This installation method is reported to give quick response times compared to open-well installations and can possibly report suctions as high as 50 kPa. The other boreholes were lined with PVC and the VW pressure transducers were suspended at depth and encapsulated by dry sand. A cap was placed atop the PVC to prevent the entry of water and other foreign matter. A slot was cut into the PVC tubing, under the cap, to allow the piezometer wires to exit. The cable exit slot was filled with silicon caulking to limit atmospheric pressure effects on the instruments. Some details of the installation are in table 4.

The values reported by the VW (or strip) piezometers require conversion to arrive at meaningful values. The raw output of a VW pressure transducer is related to the resonant frequency of the electromagnetically plucked wire. The tension on this wire changes in response to the pressure on an external diaphragm that is exposed to air and (or) fluid pressure. The resonant frequency is used in a quadratic equation, utilizing sensor specific scalars provided by the sensor manufacturer (the "ABC factors"), to convert from frequency to physical units (kPa).

Additionally, the pressure-frequency correlation of a vibrating wire is temperature dependent and requires a correction to remove temperature effects. This linear correction uses sensor manufacturer supplied values. The vibrating strip piezometer is

**Table 4.** Installation information for seven vibrating-wire piezometers. The vibrating-wire piezometers are placed in the borehole and backfilled with sand. The depth-to-sand measurement represents the distance from the ground surface to the bottom of the unscreened PVC borehole casing and the top of the sand pack.

[m, meter; NA., not available]

| Number | Borehole | Hole depth, m | Piezometer depth, m | Depth to sand, m |
|---|---|---|---|---|
| 1 | B1 | 6.04 | 0.91 | NA. |
| 2 | B1 | 6.04 | 5.03 | NA. |
| 3 | B1 | 6.04 | 5.64 | NA. |
| 4 | B1 | 6.04 | 6.04 | NA. |
| 5 | B3 | 3.14 | 3.14 | 2.74 |
| 6 | B4 | 2.96 | 2.90 | 2.44 |
| 7 | B5 | 3.60 | 3.60 | 3.05 |

more resistant to temperature variance and uses a comparatively small correction. The temperature-corrected pressure values from the piezometers are included in the dataset. Furthermore, an elevation offset of 3.7 kPa has been applied to all of the VW piezometers. It should be noted that the included value has not been corrected for barometric pressure fluctuations nor have the records been biased to a zero reference (other than that supplied by the manufacturer).

## Data Processing and Reliability

The data associated with this project are available from the USGS ScienceBase (Smith and others, 2017). The data released with this report have not undergone any significant alterations since being recorded by the data logger. The only changes consist of a voltage-to-engineering unit conversion as described in the "Methods" section. Where this process was not carried out by the data logger, it was postprocessed with MATLAB technical computing software. Empty values, such as instrument outages (see table 1), have been replaced with "not a number" (NaN).

The timestamp is represented by a decimal number originating at January 1, 0000; therefore, the initial record "732989.40625" represents November 8, 2006, at 9:45:00 a.m., coordinated universal time (UTC). Therefore, the number 732989 is the number of days since January 1, 0000, and the decimal 0.40625 multiplied by 24 hours is 9.75 hours. If the user wishes to view the data in Microsoft Excel (using a January 1, 1900, convention), the user must subtract 693,960 days from the timestamp value. Timestamps were added to missing records in order to make the record continuous (clear lapses as opposed to hidden lapses). Missing data are represented as NaN.

Although the system was monitored for reliability, there are times when sensors likely return spurious data. Attempts were made to remove gross portions of questionable data and outliers (see table 5), but careful analysis is needed to determine the accuracy of the remaining data. For example, occasionally

**Table 5.** Details of bandpass filtering for data reduction. In general, values from the dataset exceeding the limits of their expected range have been removed from the record. The filters were applied to all measurements of type unless specified otherwise.

[kPa, kilopascal; °C, degrees Celsius; VW, vibrating wire; $m^3$, cubic meter]

| Measurement type | Minimum value allowed | Maximum value allowed |
|---|---|---|
| Tensiometer pressure | –100 kPa | 10 kPa |
| Tensiometer temperature | 0 °C | 15 °C |
| volumetric water content | 0 $m^3/m^3$ | 0.6 $m^3/m^3$ |
| VW B1_4 piezometer pressure | –20 kPa | 5 kPa |
| VW B3 piezometer pressure | –6 kPa | 2 kPa |
| VW B4 piezometer pressure | –4 kPa | 0 kPa |
| VW piezometer temperatures | 0 °C | 20 °C |
| Moisture potential | 0 kPa | 500 kPa |

tensiometer and VWC data become noisy for undetermined reasons, and these data should be viewed with skepticism. These noisy data were left in the record because the overall trend in values may still be useful. The same caution in interpretation should be applied to instrumental spikes; in general, a signal trace should be smooth with multiple readings approaching a local maxima or minima. A large signal spike with no transitioning readings should be considered unreliable. Some sensors were also affected by drift. For example, continual drift can be seen in the values from piezometer 1 in B1 over its operational period. This type of error could be corrected by the use of a detrending function, but the alteration of data using "unrecoverable" techniques was not used on this dataset. The application of such techniques is at the discretion of the user.

# Summary

This report describes work completed by the U.S. Geological Survey (USGS) to investigate hydrologic response to rainfall in the landslide-prone West Hills of Portland, Oregon, from 2006 to 2017. The mountainous terrain and the marine west coastal climate of the West Hills of Portland contribute to an area with a history of landsliding, with elevated hazards occurring during rain-on-snow events. A monitoring site, installed from 2006 through 2017, quantifies annual trends in the wetting and drying of the soil and serves to further the understanding of the relationship between landslides and hydrologic triggers at this locality.

# Acknowledgments

We wish to thank Tim Corbett for his willingness to allow us to carry out this project on Mount Calvary Cemetery property. We also wish to acknowledge Raymond Surprenant and Josh Theule for the assistance they provided in field work and equipment installation.

# References Cited


Allen, J.E., 1975, Volcanoes of the Portland area, Oregon: The Ore Bin [State of Oregon Department of Geology and Mineral Industries], v. 37, no. 9, p. 145–157.

Beeson, M.H., Tolan, T.L., and Madin, I.P., 1991, Geologic map of the Portland quadrangle, Multnomah and Washington Counties, Oregon, and Clark County, Washington: State of Oregon Department of Geology and Mineral Industries Geologic Map Series GMS–75, scale 1:24:000.

Burns, S.F., Burns, W.J., James, D.H., and Hinkle, J.C., 1998, Landslides in the Portland, Oregon metropolitan area resulting from the storm of February 1996—Inventory map, database and evaluation: Oregon, Portland State University, Department of Geology, 43 p., accessed September 6, 2014, at http://nwdata.geol.pdx.edu/Landslides/PDX-Landslide/metrosld.pdf.

City of Portland, 1991, Balch Creek watershed protection plan: City of Portland, Bureau of Planning, 222 p., accessed April 21, 2015, at https://www.portlandoregon.gov/bps/article/103619.

Dyrness, C.T., 1967, Mass soil movements in the H.J. Andres experimental forest: U.S. Department of Agriculture Forest Service, Research Paper PNW–42, 12 p.

Evarts, R.C., O'Connor, J.E., Wells, R.E., and Madin, I.P., 2009, The Portland Basin—A (big) river runs through it: GSA Today, v. 19, no. 9, p. 4–10.

Harr, R.D., 1981, Some characteristics and consequences of snowmelt during rainfall in western Oregon: Journal of Hydrology, v. 53, p. 277–304.

Kizito, Fred, Campbell, C.S., Campbell, G.S., Cobos, D.R., Teare, B.L., Carter, B., and Hopmans, J.W., 2008, Frequency, electrical conductivity, and temperature analysis of a low-cost capacitance soil moisture sensor: Journal of Hydrology, v. 352, nos. 3–4, p. 367–378.

Lentz, R.T., 1981, The petrology and stratigraphy of the Portland Hills Silt—A Pacific Northwest loess: Oregon Geology, v. 43, no. 1, p. 3–10.

Lu, Ning, and Godt, J.W., 2013, Hillslope hydrology and stability: New York, Cambridge University Press, 437 p.

Madin, I.P., 1998, Earthquake-hazard geologic maps of the Portland, Oregon, metropolitan area, *in* Rogers, A.M., Walsh, T.J., Kockelman, W.J., and Preist, G.R., eds., Assessing earthquake hazards and reducing risk in the Pacific Northwest, v.2: U.S. Geological Survey Professional Paper 1560, p. 355–370.

Madin, I.P., Ma, Lina, and Niewendorp, C.A., 2008, Preliminary geologic map of the Linnton 7.5' quadrangle, Multnomah and Washington Counties, Oregon: Oregon Department of Geology and Mineral Industries Open-File Report O–08–06, 36 p., 1 map sheet, scale 1:24,000.

Mikkelsen, P.E., and Green, G.E., 2003, Piezometers in fully grouted boreholes, *in* Myrvoll, Frank, ed., Field measurements in geomechanics, Sixth International Symposium on Field Measurements in Geomechanics (FMGM), Oslo, Norway, September 15–18, 2003, Proceedings: CRC Press, 826 p.

Oregon Department of Geology and Mineral Industries (DOGAMI), 1996, Landslides in the West Hills of Portland—Preliminary look: Oregon Geology, v. 58, no. 2, p. 42–43.

Redfern, R.A., 1976, Portland physiographic inventory—A study of the physical environment and implications to planning and development: Portland, City of Portland, Bureau of Planning, 168 p.

Reese, Adam; Rhea, Chris; Block, Brian; and Burns, S.F., 2007, Facing a grave issue—Assessment of the Mt. Calvary Cemetery shopyard landslide, Portland, Oregon, January 13, 2006 [abs.], *in* The Geological Society of America Cordilleran Section Annual Meeting, 103rd, Bellingham, Wash., May 4–6, 2007, Proceedings: The Geological Society of America Abstracts with Program.

Reid, M.E., Baum, R.L., LaHusen, R.G., and Ellis, W.L., 2008, Capturing landslide dynamics and hydrologic triggers using near-real-time monitoring, *in* Chen, Zuyu; Zhang, Jianmen; Li, Zhongkui; Wu, Faquan; and Ho, Ken, eds., Landslides and engineered slopes—From the past to the future: London, Taylor and Francis Group, p. 179–191.

Schlicker, H.G., 1956, Landslides: The Ore Bin, v. 18, no. 5, p. 39–43.

Smith, J.B., Godt, J.W., Baum, R.L., Coe, J.A., Ellis, W.L., and Burns, S.F., 2017, Results of hydrologic monitoring of a landslide-prone hillslope in Portland's West Hills, Oregon, 2006–2017: U.S. Geological Survey data release, https://doi.org/10.5066/F7KK98XK.

Smith, J.L., 1974, Hydrology of warm snowpacks and their effects upon water delivery—Some new concepts, *in* Santeford, H.S., and Smith, J.L., comps., Advanced concepts and techniques in the study of snow and ice resources—An interdisciplinary symposium, Monterey, Calif., December 2–6, 1973: Washington, D.C., National Academy of Sciences, p. 76–89.

Swanston, D.N., 1974, Slope stability problems associated with timber harvesting in mountainous regions of the western United States: U.S. Department of Agriculture Forest Service, General Technical report PNW–GTR–21, 19 p.

Taylor, G.H., 1997, The great flood of 1996—Its causes and a comparison to other climate events, *in* Vomocil, J.A., ed., Stream temperatures, flood impact, public health issues, and nutrient management, Proceedings of the James A. Vomocil Water Quality Conference, Corvallis, Oregon, 1996: Oregon Water Resources Research Institute, Oregon State University Extension Service, Special Report 970, p. 2–6.

Taylor, G.H., and Bartlett, Alexi, 1993, The climate of Oregon, climate zone 2, Willamette Valley: Corvallis, Oregon State University, Oregon Climate Service, Special Report 914, 5 p.

Treasher, R.C., 1942, Geologic history of the Portland area: State of Oregon Department of Geology and Mineral Industries, GMI Short Paper No. 7, 17 p., 1 map sheet, scale 1:250,000.

Trimble, D.E., 1963, Geology of Portland, Oregon, and adjacent areas—A study of Tertiary and Quaternary deposits, lateritic weathering profiles, and of Quaternary history of part of the Pacific Northwest: U.S. Geological Survey Bulletin 1119, 125 p.

U.S. Department of Agriculture Natural Resources Conservation Service, 2014, Web soil survey: U.S. Department of Agriculture, Natural Resources Conservation Service, accessed September 6, 2014, at http://websoilsurvey.nrcs.usda.gov/.

Varnes, D.J., 1978, Slope movement types and processes, *in* Schuster, R.L., and Krizek, R.J., eds., Landslides—Analysis and control: Washington, D.C., Transportation Research Board, National Research Council, Special Report 176, p. 11–33.

Walsh, Ken, Peterson, G.L., Beeson, M.H., Wells, R.E., Fleck, R.J., Evarts, R.C., Duvall, Alison, Blakely, R.J., Burns, Scott, 2011, A tunnel runs through it—An inside view of the Tualatin Mountains, Oregon: U.S. Geological Survey Scientific Investigations Map 3144.

Wiley, T.J., 2000, Relationship between rainfall and debris flows in western Oregon: Oregon Geology, v. 62, no. 2, p. 27–43.

Publishing support provided by:
Denver Publishing Service Center, Denver, Colorado

For more information concerning this publication, contact:

Center Director, USGS Geologic Hazards Science Center
Box 25046, Mail Stop 966
Denver, CO 80225
(303) 273-8579

Or visit the Geologic Hazards Science Center website at:
https://www.usgs.gov/centers/geohazards

This publication is available online at:
https://doi.org/10.3133/ds1050

ISSN 2327-638X (online)
https://doi.org/10.3133/ds1050